INSIGHTS INTO HYDROXYL/WATER STABILITY AND FORMATION IN THE MAIRAN CRATER REGION FROM M³ GLOBAL/TARGET MODE DATA. F. Colaiuta[1,2], F. Tosi[2], F. Zambon[2], G. Pratesi[3,2], M. Anand[4], and M. Boruah[4]. [1]Dipartimento di Fisica, Sapienza Università di Roma, Rome, Italy. [2]Istituto Nazionale di Astrofisica – Istituto di Astrofisica e Planetologia Spaziali (INAF-IAPS), Via del Fosso del Cavaliere, Rome, Italy. [3]Dipartimento di Scienze della Terra, Università degli Studi di Firenze, Florence, Italy. [4]School of Physical Sciences, The Open University, Robert Hooke Building, Kents Hill, Milton Keynes, United Kingdom

Introduction: Hydration on the Moon, in the form of OH/H_2O, has been recognized as a global scale phenomenon [1,2]. However, its behavior at local scales and across the lunar diurnal cycle remains poorly constrained. The Mairan crater region (~41.6°N, 44.5°E; Figure 1a) represents an interesting case study, owing to reported hydrogen anomalies and the rare availability of spatially and temporally overlapping imaging spectroscopy datasets, acquired by the Chandrayaan-1/Moon Mineralogy Mapper (M³) in both global-mode and target-mode observations [3,4].

Methods and data: We performed our analysis on high-quality M³ observations acquired during the OP1B (global-mode, ~08:15 LST) and OP2A (target-mode, ~15:40 LST) mission phases to maximize radiometric stability [4] and allow diurnal cross-comparisons (Figure 1b). Resulting reflectance spectra were photometrically corrected using the standard M³ team pipeline [4] and then smoothed with a Savitzky–Golay filter. Thermal residual effects were handled with three independent removal schemes: (i) the empirical approach of Clark et al. (2011) [5], (ii) the semi-empirical channel-ratio method of Li & Milliken (2016) [6], and (iii) a roughness-aware model partially starting from Wohlfarth et al. (2023) [7].

To relate hydration to surface properties, we computed multiple spectral indices and performed Fully Constrained Least Squares (FCLS) unmixing over the 0.7–2.3 μm range. OH/H_2O abundance was estimated using the *Effective Single-Particle Absorption Thickness* (ESPAT), which is linearly correlated with OH/H_2O content [8] and retrieved via Hapke's radiative transfer model [9]. Finally, for target-mode data we applied a K-Means cluster-based analysis to overcome SNR limitations [10] and to better separate distinct terrain units.

Results from spectral indices and unmixing: Cluster analysis of M³ target-mode observations identifies seven distinct spectral units (Figure 2) and shows a robust connection between diagnostic absorptions and hydration trends. In the early morning, the hydration band appears broad and displaced toward ~2.85 μm. However, the instrument's spectral resolution and the temperature sensitivity of the band shape prevent a definitive interpretation of the apparent shift. By mid-afternoon, the absorption evolves into a narrower, well-defined feature centered near ~2.75 μm, consistent with structurally bound OH in defect-rich silicates and indicating preferential retention of solar wind–implanted protons in specific hosts [11].

Additional compositional insight comes from the 2 μm region: surfaces with weaker and broader 2 μm absorptions tend to exhibit higher hydroxyl abundances (Figure 3). This pattern is typical of agglutinate-rich soils, where the amorphous glass component suppresses and broadens pyroxene bands. In line with this, FCLS unmixing reveals a positive relationship between hydroxyl and agglutinate fraction, supporting the idea that agglutinates act as efficient long-term reservoirs. In contrast, we find no meaningful correlation with the OMAT index [12], implying that hydration persistence is controlled by the microstructural characteristics of regolith phases.

Diurnal variability and comparison with lunar samples: Comparing early-morning and mid-afternoon observations shows pronounced diurnal variability in hydration across our study area. In the morning (~08:15 LST, global-mode), OH/H_2O abundances are relatively high and widespread (~140–450 ppm). These values depend on the assumed grain size [8], here constrained to 0–75 μm by FCLS results, and under cooler conditions hydration appears broadly distributed with limited selectivity.

By mid-afternoon (~15:40 LST, target-mode), water is lost and hydroxyl drops to ~30–100 ppm, corresponding to a 60–80% decrease. These levels match hydration measured in agglutinates from Apollo and Chang'e 5 samples [13, 14], supporting the view that space-weathered glasses are the main hosts of structurally bound hydroxyl at higher temperatures. Hydration also becomes more localized, persisting chiefly in agglutinate-rich terrains where defect-rich glass can retain protons against thermal desorption.

Unmixing in the 2.5–3.0 μm interval is consistent with this picture: crushed silica and irradiated Apollo analogs (LS78421 and LS73131) [15] best reproduce the ~2.75 μm band, while endogenous components remain negligible within uncertainties.

Conclusions: This work provides one of the first detailed local-scale constraints on the diurnal hydration cycle at Mairan using overlapping M³ global and target-mode observations. Our results reveal a dual hydration regime: in the early-morning, OH/H_2O is widespread but transient, while in the mid-afternoon only a smaller,

stable fraction remains, preferentially hosted in agglutinate glasses. The strong correlation between ~2.75 µm band depth and agglutinate abundance shows that regolith microstructure, rather than bulk composition or optical maturity, controls hydration stability. The observed diurnal decrease (60–80%) underscores the dynamic nature of lunar hydration and confirms its primarily exogenous origin. This framework refines our understanding of volatile behavior at mid-latitudes local scale and highlights agglutinates as key reservoirs for stable hydroxyl.

Acknowledgments: The authors acknowledge support from the Space It Up project, funded by the Italian Space Agency and the Italian Ministry of University and Research. Contract n. 2024-5-E.0 – CUP n. I53D24000060005.

References:

[1] Pieters (a), C.M. et al. (2009) *Science, 326(5952), 568-572.*
[2] Clark, R.N. (2009) Science, 326(5952), 562-564.
[3] Pieters (b), C.M. et al. (2009) *Current Science, 96(4), 500-505.*
[4] Green, R.O. et al. (2011) *Journal of Geophysical Research, Planets, 116(E10).*
[5] Clark, R.N. et al. (2011) *Journal of Geophysical Research, Planets, 116(E6).*
[6] Li, S. & Milliken, R.E. (2016) *Journal of Geophysical Research, Planets, 121(10).*
[7] Wohlfarth, K. et al. (2023) *Astronomy & Astrophysics, 674(A69).*
[8] Li, S. & Milliken, R.E. (2017) *Science Advances, 3(9).*
[9] Hapke, B. (1984) *Icarus, 59(1), 41-59.*
[10] Clark, R.N. et al. (2024) *The Planetary Science Journal, 5(9).*
[11] McLain, J.L. et al. (2021) *Journal of Geophysical Research: Planets, 126, e2021JE006845.*
[12] Lucey, P.G. et al. (2000) *Journal of Geophysical Research, Planets, 105(E8).*
[13] Liu, Y. et al. (2012) *Nature Geoscience, 5, 779–782.*
[14] Zhou, C. et al. (2024) *Science Advances, 10(19), eadl2413.*
[15] Yeo, L.H. et al. (2025) *Journal of Geophysical Research, Planets, 130(E3).*

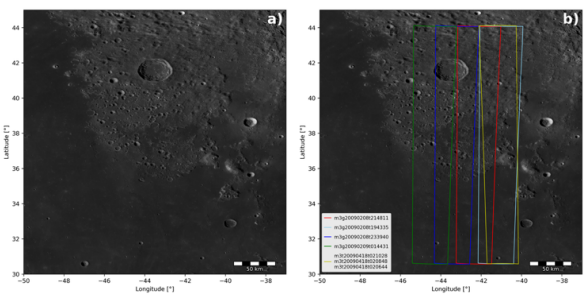

Figure 1: Mairan crater region from the LROC/NAC (a) and the M^3 datasets used for this work (b).

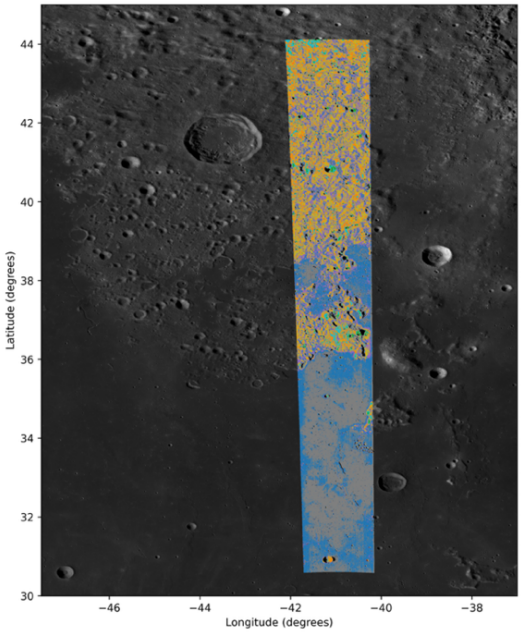

Figure 2: Clusters derived from the K-Means algorithm. Within the overlapping area for global and target-mode data (Figure 1b), seven units are identified: Oceanus Procellarum (OP1 and OP2) and Mairan Peninsula (MP1, MP2, MP3, MP4 and MP5) clusters.

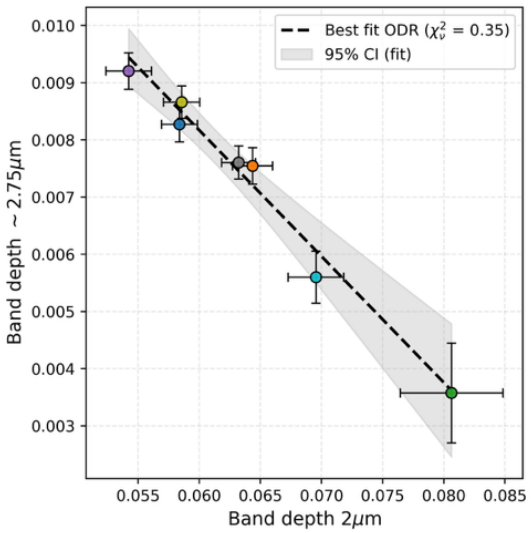

Figure 3: The depth of the ~2.75µm band is examined in relation to the ~2.0µm band depth for the Li&Milliken [6] thermal removal method. Color scheme is the same of Figure 2. The two indices show a correlated trend, as indicated by the best-fit regression (black dotted line). The same trend is observed for Clark and Wohlfarth thermal removal methods [5,7].